The New Protective Anti-graffiti Coatings for Railway Vehicles and a Proposal for a Quantitative Method for Selecting the Best Varnish

Norbert Radek , Ewa Kozień , Łukasz Pasieczyński , Łukasz Jan Orman , Marek S. Kozień *

Posted Date: 12 May 2025

doi: 10.20944/preprints202505.0859.v1

Keywords: anti-graffiti coatings; cost analysis; railway transport; sustainable development

 doi:10.20944/preprints202505.0859.v1

Article

The New Protective Anti-graffiti Coatings for Railway Vehicles and a Proposal for a Quantitative Method for Selecting the Best Varnish

Norbert Radek [1], Ewa Kozień [2], Łukasz Pasieczyński [3], Łukasz J. Orman [4] and Marek S. Kozień [5,*]

[1] Kielce University of Technology, Faculty of Mechatronics and Mechanical Engineering
[2] Krakow University of Economics, College of Management and Quality Sciences
[3] Firma Handlowa BARWA Jarosław Czajkowsk
[4] Kielce University of Technology, Faculty of Environmental Engineering, Geomatics and Renewable Energy
[5] Cracow University of Technology, Faculty of Mechanical Engineering
* Correspondence: marek.kozien@pk.edu.pl

Abstract: The unexpected appearance of graffiti on rail vehicles and the need to remove it is an increasingly serious problem for rail carriers, also due to costs. The use of anti-graffiti protective coatings by rail companies is becoming more and more common. These coatings must meet appropriate quality requirements, in particular regarding their mechanical properties and features, such as: roughness, waviness, adhesion, hardness. The use of anti-graffiti coatings is also associated with the technology of their production and removal, taking into account the problem of environmental impact and costs. Some of anti-graffiti coating systems were tested and compared. Anti-graffiti coating systems were characterized by low parameters of the geometric structure of the surface and good adhesion. Moreover they had good mechanical properties and were free of structural defects as pores or microcracks. Anti-graffiti paint systems were characterized by hydrophobicity, which helps reduce the adhesion of undesirable substances on their surfaces. Also discussed are various aspects of the costs incurred by railway companies due to the existence and removal of graffiti from passenger cars. Economic analyses included data from Polish and Spanish national and regional railway companies . Moreover the article proposes an original method of selecting of the anti-graffiti coatings.

Keywords: anti-graffiti coatings; cost analysis; railway transport; sustainable development

1. Introduction

Among problems, the incidence of which is systematically increasing, and in particular applies to rail transport is the removal of the consequences of vandalism, which is the problem of destruction of train cars, especially passenger trainsets, by graffiti painting, which has become a challenge for many railway companies in Europe, including Poland, in the 21st century. In the article [1] the problem of costs incurred by rail carriers in the world (in Germany, Spain, Belgium, the Netherlands, Australia) is discussed. Some of the economic and management aspects that throw quantitative and cost dimensions of the problem are briefly presented in a separate section 2. The analysis of costs of anti-graffiti removal is not the main research axis of the article, but it is important in the overall view of the research problem of graffiti removal, just as, for example, in the article [x] the economic analysis performed also had the character of extending the research from the point of view of practical applications. Graffiti found on railcars violates the exterior aesthetics of trains and lowers the element of distinction of the network operator and the type of vehicle. Nowadays, during vehicle production, rolling stock manufacturers are required to apply an anti-graffiti coating in addition to painting the exterior plating. Polish rolling stock manufacturer PESA has been using such coatings since 2004 [3]. The paint coating of Elf2 railbuses ordered for Małopolska in PESA is mandatory to be covered with

 doi:10.20944/preprints202505.0859.v1

a special layer that prevents the application of graffiti and is supposed to fulfill its properties for the shortest period of 10 years [4]. It is important that the coating is made in accordance with the technological and production process of the vehicle manufacturer. Vehicle manufacturers indicate that the parameters of the paint coating are maintained when the anti-graffiti coating is painted ten times and the graffiti paint is removed using the appropriate procedure with dedicated agents. They further state that the amount of cleaning of the graffiti surface, as well as the impact of graffiti, i.e. the degree of damage to the paint coating, depends primarily on the type of paint and graffiti coating materials, the length of time the graffiti remains on the vehicle paint surface, from the application until the graffiti surface is washed off, and the atmospheric conditions, ambient temperature, humidity, sunshine, precipitation affecting the applied graffiti. All repair, renovation work is carried out in the repair hall, maintaining appropriate temperatures, in pollution-free conditions. The materials used to repair paint coatings must meet the conditions in accordance with the manufacturer's technology. Anti-graffiti coatings are being modified by manufacturers on an ongoing basis, following the fact that graffiti paints are also becoming more aggressive. The chemical company BARWA has developed a new family of anti-graffiti coatings. The article presents analyses concerning the study of required properties that these coatings should meet. This research was related to the PhD thesis [5].

The properties of the surface layer affect the service life of machinery and equipment. The surface fundamentally affects the performance of objects and products. A number of physicochemical phenomena such as chemical catalysis, corrosion, wear (abrasive, adhesive, abrasive-adhesive, erosive, cavitation, fatigue), adhesion, adsorption (physical and chemical), flotation, depend on and take place on the surface of the material or with its participation [6, 7]. Coatings are simultaneously affected by various types of factors: thermal and corrosive (alkalis, acids and salts), moisture and solar radiation in the form of destructive UV radiation, whose influence on the destruction process of coatings is synergistic [8, 9]. The impact of operating environment factors has a significant effect on the condition of the surface of polymer coatings. As a result of adsorption of aggressive substances on the surface of coatings, as well as the impact of ultraviolet radiation, intensive chemical and physical destruction of the surface of coatings occurs, primarily deteriorating their decorative properties [10-13]. The penetration of aggressive media into the interior of polymer coatings can also cause swelling and blistering - as a result of the accumulation of media near the substrate and due to the development of subsurface corrosion [14]. The effects of the influence of aggressive substances increase if the polymeric material has also been subjected to the influence of other operating factors, such as heat, mechanical loads, including the impact of erosion particles (hail, sand, clods of earth, stones) [15]. From the moment the application process is completed, the coating is exposed to destructive operating factors. One of the most dangerous factors destroying polymer coatings are aggressive media (acid rain, brine, battery acid), causing destruction of their chemical structure through: leaching, hydrolysis, or oxidation [16-19]. In the initial stage of destruction there is a deterioration of the decorative properties of coatings (dulling, color change, loss of gloss), while in its final stage the aggressive media migrating deep into the coating cause corrosion wear of the substrate [20]. When aqueous solutions of sodium chloride affect the paint coating, the first stage of its destruction process is the formation of conductive paths (capillaries), which allow direct access of chloride ions to the surface of the metal substrate [17, 18, 20]. The rate of diffusion of aggressive media in polymer coatings decreases as the number of layers increases. Anticorrosion properties of organic coatings is presented in [21]. The influence of the surface texture of dedicated composite for wet painting, on durability of gloss parameters and colour [22]. Various strategies and methods are considered to eliminate graffiti from rail vehicles. In article [1] is presented the original ultra-freezing air projection method. While in the article [23] the environmentally safe graffiti remover is proposed.

Initially, paint coating systems were designed to protect the surface of steel from aggressive external agents and to impart color. With the help of paint coatings, special effects and properties began to be imparted to the vehicles to which these systems were applied. One such system with special properties is the protective anti-graffiti coating system. When we talk about a protective

 doi:10.20944/preprints202505.0859.v1

coating system that includes a clear anti-graffiti coating we are actually talking about a coating that gives the ability to easily remove unwanted subsequent layers of paint without damaging the original paint layer. This can be achieved by using a highly chemically and mechanically resistant coating or by giving it properties that reduce the adhesion of subsequent layers. Reduced adhesion means that it is easier to remove anything that is found on the surface of the structure: dust, acidic or alkaline deposits, but also graffiti paint. The use of special anti-graffiti coating systems helps reduce vandalism on rolling stock and speeds up the process of removing damage caused by graffiti. For this purpose, less aggressive cleaning agents should be used, which ultimately contributes to environmental protection and reduces the losses that are incurred as a result of railway vehicles (wagons) downtime.

The aim of the article is to present the new family of coatings designed by BARWA company, pointed out the results of laboratory tests of properties of parameters important from the point of view of operation of railway wagons. Moreover the article proposes an original method of selecting of the anti-graffiti coatings.

2. Costs of anti-graffiti removal

When analyzing the economic aspects of destroying train depots by painting graffiti, the problem should be looked at holistically, taking into account the technological aspect discussed earlier, but also the ecological, social, managerial, as well as legal aspect.

Most of them involve large additional costs for rail companies. For example, at the moment, the cost of repairing a damaged EN57-type depot alone is in the range of 6000÷8000 EUR. The cost of removing graffiti from railroad cars includes: material costs, energy costs, direct labor costs. In the case of damage to the paint coating on the vehicle, taking into account the mechanical damage to the paintwork caused by repeated acts of vandalism (several times applied and removed layers of pseudo-graffiti with violation and mechanical destruction of both the paint and the performed undercoat), estimated in terms of the required materials as well as labor intensity in accordance with the current processes of repair and restoration of paint, converted for one square meter of the repaired area is about 200 EUR net. This cost is an estimate, it does not take into account the significant costs of taking the vehicle out of service and stopping it to perform graffiti removal activities, but essentially takes into account the following scope of work:

Verification, determination of the area of repair, taping and protection of the bordering surfaces;

Repairing the occurring mechanical damage, scratches, degreasing, sanding, polishing and dust removal, and making the repair layer;

Selecting the color scheme, taking into account the shades of the adjacent surfaces of the base paints, and carrying out the renovation with the base paints for the given paint surface, taking into account the drying and evaporation times;

Restoration of damaged inscriptions, descriptions, decals;

Applying a new layer of anti-graffiti clearcoat to the entire repaired surface;

Removal of protections, polishing, washing of repaired surfaces.

In order to illustrate the problem, data from selected years relating to Polish National Railway Company (PKP), Polish regional railway companies (Mazovia Railways, Silesian Railways, Małopolska Railways) and the national rail company in Spain - Renfe Operadora (RENFE La Red Nacional de Ferrocarriles Españoles) - are summarized. Table 1 summarizes the costs incurred by the carriers in selected years for the specified operations related to the removal of graffiti from railcars. Table 2 summarizes the areas of railcars damaged by graffiti, while Table 3 lists the number of acts of vandalism.

Table 1. Costs incurred by railway companies (in thousand PLN).

Year	Company	Activity	Cost (kPLN)	Source
2001	PKP Railways	Removal of graffiti	227	[24]
2017	Mazovia Railways	Removal of graffiti	1 700	[25]

 doi:10.20944/preprints202505.0859.v1

2018	Silesian Railways	Removal of graffiti	60	[25]
2022	RENFE Railways	Total graffiti costs	100 000	[26]
2021	Malopolska Railways	Removal of graffiti	37	own
2022	Malopolska Railways	Removal of graffiti	121	own
2023	Malopolska Railways	Removal of graffiti	200	own

Table 2. The area of the surface of graffiti being removed (in thousands of square meters)

Year	Company	Area (km²)	Source
2017	Mazovia Railways	11	[25]
2018	Mazovia Railways	8	[25]
2018	RENFE Railways	80	[26]
2021	Malopolska Railways	0.4	own
2022	Malopolska Railways	0.9	own
2023	Malopolska Railways	1	own

Table 3. Total number of graffiti acts of vandalism

Year	Company	Number	Source
2018	Silesian Railways	40	[25]
2022	RENFE Railways	3559	[26]
2021	Malopolska Railways	39	own
2022	Malopolska Railways	44	own
2023	Malopolska Railways	50	own

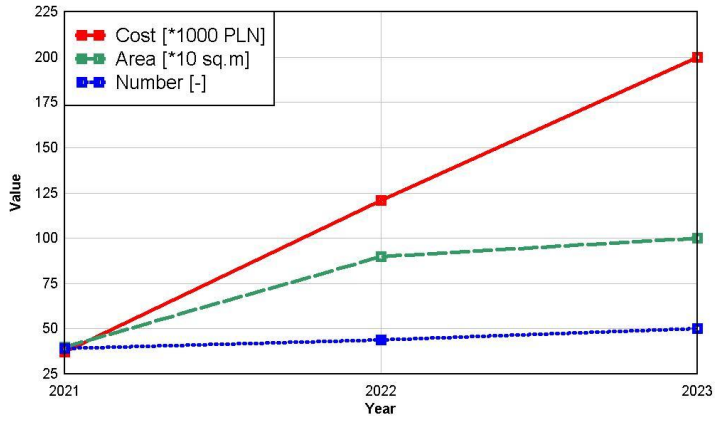

Figure 1. Trend in costs, areas and number of cases for the Malopolska Railways.

The upward trend in the cost, area and number of cases of graffiti removal for the Malopolska Railways in 2021-2023 is shown in the graphs in Fig. 1. There is an increase in the number of cases by 28% over the two years analyzed, as well as a 150% increase in the area subjected to renovation (graffiti removal). On the other hand, the cost of renovation has increased more than five times. This means, the need for widespread use of atygraffiti coatings and rapid removal of graffiti.

It is worth noting the difficulties faced by preventive measures. Despite the costs incurred for the system of monitoring and protection of rolling stock in 2022, the Spanish carrier RENFE recorded 3559 incursions by graffiti artists into railroad areas, and only in 729 cases was it possible to prevent vandalism. Some of the apprehended vandals have been punished in court proceedings conducted. The painting of trains also affects subway depots. For example, in February 2023, in the morning

 doi:10.20944/preprints202505.0859.v1

hours at a subway station, vandals painted a subway depot by blocking the depot's movement with an emergency brake beforehand [27], in August 2023, at night at a subway station, a group of masked vandals painted a subway train by stopping its movement with an emergency brake beforehand [28], and in December 2023, at night at a subway station, 10 vandals painted a subway train almost its entire length in less than five minutes [29].

An analysis of the cost of removing graffiti from railway vehicles or wagons requires investment in an effective system for monitoring and protecting oil rolling stock, which must be combined with a civic-minded public. On the other hand, the failure to take systemic and preventive measures, as well as the failure to reduce the scale of graffiti vandalism, will result in an increase in the cost of removing graffiti from train depots following an increase in the price of anti-graffiti paints and labor costs.

3. Materials and Methods

3.1. Protective coatings

A coating system with special properties is a protective anti-graffiti coating system. The main purpose of using this coating is to protect the surface of the structure from corrosion. The use of joint compound makes it possible to improve the shape of the structure resulting from heat transport during welding work in the production process. To give the aesthetics desired by the customer - in the form of color, gloss or special decorative effects (hammer effect, crease effect). The end result is the protection of the vehicle from the end user in the form of a specialized anti-graffiti layer. The protective system fulfills its function if it adheres tightly to the vehicle surface and maintains its continuity. When graffiti paint appears on the protective coating, physical and, in some cases, chemical changes occur in the coating. By physical changes we mean the diffusion of solvents and the carrier medium included in graffiti varnishes. Such a coating, due to interaction with chemical solvents such as acetone, xylene, mesylene, butyl acetate, ethyl acetate and solvent mixtures (toluene solvent, white spirit, nitro), can be destroyed. In the first stage, solvents can migrate deep into the coating and cause it to soften. In subsequent stages, such a coating may become fluffed up, cracked and even delaminated. The damage will mainly depend on the aggressive components of the graffiti paint. In addition, the conditions in which the vehicle is located, such as high sunlight resulting in the heating of the vehicle, combined with aggressive solvents in the graffiti paint can have a devastating effect on the protective coating. Another key parameter is time, in order not to allow graffiti to contact the protective coating for too long, the composition is immediately taken out of service and directed to washing. Contaminants that have more firmly “bonded” to the surface of the clearcoat can be removed chemically or mechanically, while being aware of the gradual damage to the clearcoat. Such actions can lead to a reduction in the thickness of the clearcoat (with a dry film thickness of about 40÷60 μm). After several repetitions of such a process, the basecoat may be exposed. The entire system will then be significantly weakened, which will directly affect its aesthetics and the component's susceptibility to corrosion. This can lead to a situation where it will be necessary to carry out refinishing ahead of schedule, this will generate unnecessary costs. It seems reasonable to use such a clearcoat to protect the system from external influences as much as possible. The clearcoat that finishes the system should also exhibit special characteristics, such as reduced adhesion of subsequent layers and their eventual easy removal.

3.2. Anti-graffiti coatings laboratory tests

The way the paint system is made has a major impact on the vehicle's service life. The performance tests compared three paint systems based on anti-graffiti coatings from PPG (the world's leading paint manufacturer) with a paint system that included BO100-AGR paint coating (developed in the laboratory of Firma Handlowa Barwa Jarosław Czajkowski). The following anti-graffiti coating

 doi:10.20944/preprints202505.0859.v1

systems were considered in laboratory tests: XPC 60012, XPC 60011, XPC 60036 and BO100-AGR with the properties given in Table 4.

Table 4. Physical parameters of the coating systems used in tests

Material	Mass density [kg/m³]	Weight proportion
XPC60011	990	1:1
XPC60012	980	3:1
XPC60036	1010	2:1
BO100-AGR	1020	2:1

Each coating system consisted of an epoxy anti-corrosion primer, polyester putty, polyurethane filler, an aesthetic base coat and a colourless anti-graffiti varnish applied to an alloy steel core. The compositions of the individual layers were not given due to the trade secrets of the manufacturers (PPG and Firma Handlowa Barwa Jarosław Czajkowski).

In order to compare different anti-graffiti coating systems with each other and determine their suitability, the performance properties of the coating system (mechanical properties, physical-chemical properties) were selected, which translate into an assessment of their service life and cost of performance. The test speciments were made of the S355 alloy steel. The surface preparation and coating (painting) procedure was strictly defined and repeatable for all samples and coatings applied. The procedure was described in detail in [30].

On the basis of our own research, the following parameters for the application of on anti-graffiti coatings were assumed:

- application technique: pneumatic spray,
- application: four layers,
- surface temperature: 21-23 °C,
- operating pressure: 0.20-0.22 MPa,
- evaporation time between layers: 20 minutes,
- evaporation before baking: 20 minutes,
- annealing temperature: 50 °C,
- annealing time: 60 minutes,
- thickness of dry film: 40-50 μm.

The remaining layers were applied in accordance with the technical data sheets recommended by the manufacturers.

3.2.1. Microstructural analysis

Samples for metallographic testing were cut using an ISOMET cutting machine. The cut specimens were then embedded in BUEHLER KonductoMet thermosetting conductive resin using a BUEHLER SimplyMet 3000 inlay press. The metallographic specimens were ground on a BUEHLER MetaServ 250 grinder on water papers with grain gradations from 80 to 2500, each time changing the angle by 90° to the direction of the scratches from the previous paper gradation. Polishing of the specimens was carried out on a BUEHLER EcoMet 250 grinder-polisher with pneumatically adjustable pressure and speed. The specimens were polished on MicroDiamant Mambo cloth in MicroDiamant O.P.S suspension 0.05 μm. The metallographic specimens prepared in this way were subjected to microscopic observations. A JEOL type JSM-7100F field emission scanning electron microscope (SEM) was used to study the microstructure.

The photograph (Fig. 2) shows an example of the micro-structure of the BO100-AGR anti-graffiti coating system. Based on the results, the minimum thickness of the anti-graffiti coating was about 42 μm, while the maximum thickness was about 43 μm.

 doi:10.20944/preprints202505.0859.v1

SEM analysis showed that the thickness of the basecoat layer was between 18-19 μm. The undercoat layer had a thickness in the range of about 50 μm to 55 μm. The layer with putty had the greatest thickness of about 2210÷2250 μm. Clear boundaries between the individual layers can be seen (Figure 1). In addition, Figure 2 shows a clear boundary between the paint layers and the putty. We can also observe that the paint layers are free of pores and micro-cracks. Analyzing the morphology of the other anti-graffiti coating systems XPC 60011, XPC 60036, BO100-AGR, it was found that the thicknesses of the individual layers are comparable to the thicknesses of the layers of the XPC 60012 anti-graffiti coating system. The thickness of the anti-graffiti coating systems produced ranged from about 2300 to about 2400 μm.

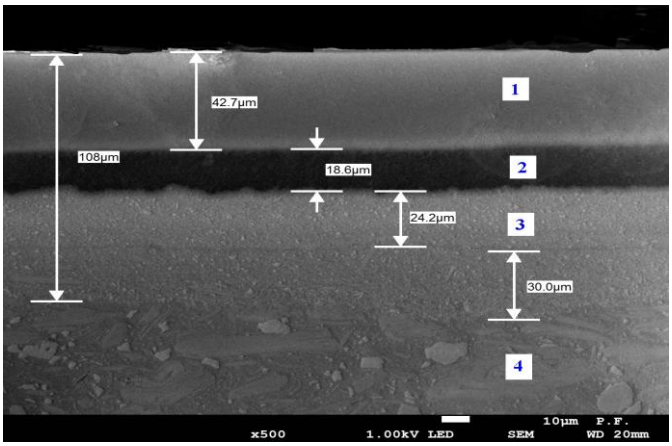

Figure 2. SEM micrographs of the polished cross-section throug a anti-graffiti BO100-AGR coating system on steel substrate: 1- anti-graffiti layer, 2 - base layer, 3 - undercoat layer, 4- putty.

3.2.2. Measurement of surface free energy

So far, a method for direct measurement of surface free energy (SFE) has not been developed. For this purpose, an indirect method is used, based on measuring the angle of wetting of surfaces by reference liquids, and then using mathematical models, the surface free energy is calculated.

Determination of the wetting angle of the surface of structural materials was used according to a method based on the geometry of the droplet. The surface of the droplet is most often shaped like a bowl, and then the wetting angle is calculated from measuring the height of the bowl h and the radius of the droplet's contact area r. The canopy height is given by the formula h = R(1 - cosQ), and the surface contact radius r=RsinQ. From these relationships, we get equation (1) [1], where: θ - angle of wetting of the surface, h - height of the canopy, r - the radius of the droplet contact surface.

$$\Theta = \frac{2h}{r} \quad (1)$$

The value of the surface free energy of structural materials is determined indirectly using the measurement of wetting angles with selected measuring fluids. Distilled water and diiodomethane (DIM) were used as measuring fluids for measuring the wetting angle. A stereoscopic microscope with a camera and MicroScan v 1.3 software were used to observe the droplets and measure the wetting angle.

The following values of the surface free energy constants of the measuring fluids and their polar and dispersive components were adopted: gw=72.8 [mJ/m²], gpw=51.0 [mJ/m²], gdw=21.8 [mJ/m²], gd=50.8 [mJ/m²], gpd=2.3 [mJ/m²], gdd=48.5 [mJ/m²]. The measuring liquid was applied to the test surface using a micropipette with a fixed volume of 5 μl.

The surfaces of the polymers that were studied are polar in nature, so in this case the SFE calculated by the Zisman method is not appropriate. The Owens-Wendt method is commonly used to determine the surface free energy of composite materials in which the surface free energy is

 doi:10.20944/preprints202505.0859.v1

assumed to be the sum of two components: dispersive and polar (2) [1]: where: γdS - dispersive component of surface free energy, γpS - the polar component of the surface free energy.

$$\gamma_s = \gamma_s^d + \gamma_s^p \quad (2)$$

The measurement series consisted of measurements of the wetting angle of ten successively injected drops of liquid onto the surface of the paint system. The measured wetting angle of the coating system by a given liquid was used to calculate the surface free energy. The same methodology was used to test each anti-graffiti coating system. Taking ten measurements for each coating system allowed the test results to be averaged.

Figure 3 compares the surface free energy of the anti-graffiti coating systems tested. In order to achieve reduced contaminant adhesion of the protective layer, the free surface energy is sought to be minimized. The lowest surface free energy values were shown by the XPC60011 and BO100-AGR coating systems. From the point of view of rolling stock and anti-graffiti protection, these two systems had the desired properties. The aforementioned anti-graffiti paint systems were characterized by hydrophobicity, which is conducive to reducing the adhesion of undesirable substances on their surfaces. However, it should be borne in mind that graffiti paints consist of various resins, fillers, pigments and additives, so synergistic interactions may occur, so it is difficult to predict the exact mechanism of interaction between hydrophilic and hydrophobic surfaces. As the wettability of the material increases (smaller wetting angle), more work needs to be done to disconnect the surface of the coating system from contaminants formed on the surface. The more hydrophobic the material was, the greater the wetting angle, and the smaller the adhesion work.

Figure 4 shows the surface free energy of the anti-graffiti coating systems tested, divided into dispersive and polar components. It is noteworthy that the dispersion component contributed the most to the increase in the total SFE value. The XPC 60011, XPC60012 and XPC60036 paint systems were characterized by a similar value of the dispersion component. However, in the case of the XPC 60011 coating system, the reduced adhesion of graffiti varnishes was achieved by reducing the polar component of SFE.

The polar component is the sum of components derived from interactions between molecules, including polar, inductive, hydrogen, acid-base interactions. Dispersive interactions, on the other hand, represent the dispersive component of surface free energy. Modification of the developed BO100-AGR coating system leads to a reduction in the value of surface free energy. This is primarily associated with a decrease in its dispersion component, compared to the other coating systems studied. By chemically modifying the SEP between contacting phases, larger wetting angles can be achieved with unwanted substances. On the other hand, by modifying the surface of the material with a chemical substance, the chemical composition, structure, or roughness of the surface layer is changed, resulting in changes in interfacial interactions. For these reasons, only results obtained by the same method and using the same measuring fluids can be the subject of comparative analyses of SFE values.

 doi:10.20944/preprints202505.0859.v1

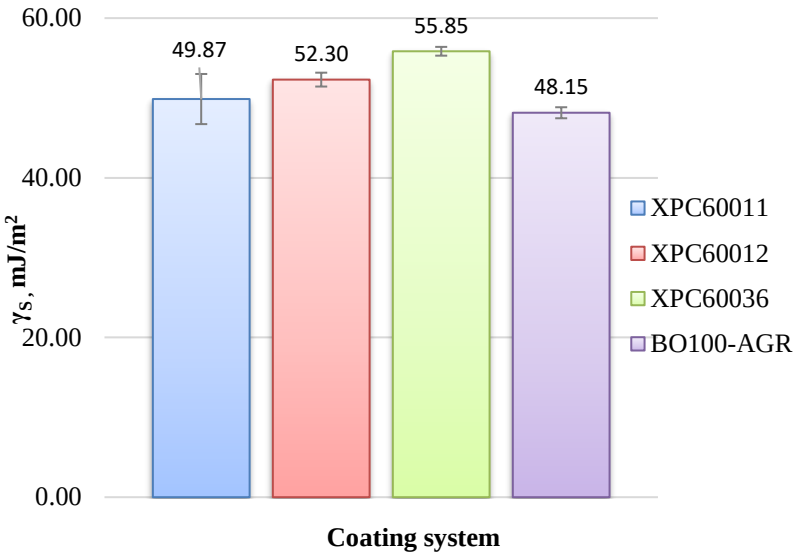

Figure 3. Comparison of the total surface free energy of the tested systems anti-graffiti coatings.

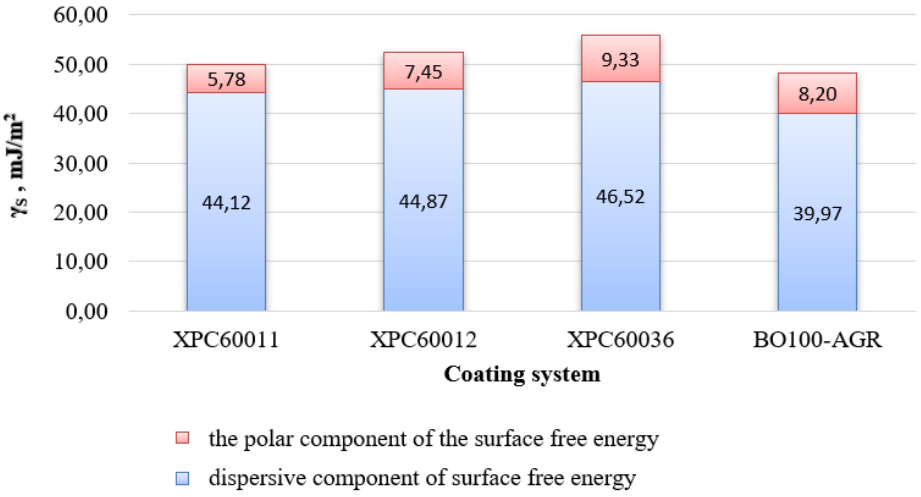

Figure 4. Comparison of the components of the total surface energy of the tested systems anti-graffiti coatings.

Further research work should determine whether SFE changes during operation or remains constant. Also of interest is the change in surface free energy after successive cycles of both vehicle washing and graffiti paint washing. However, when conducting studies to determine the degree of degradation and kinetics of change under the influence of external factors, it should be borne in mind that simulating the external environment yields approximate results, and verification of the error is only possible by conducting independent tests on a real sample.

The example is proof of the great importance of SFE in the process of creating polyurethane protective coatings that meet the requirements of modern materials engineering.

Based on the obtained results statistical analysis of surface free energy of anti-graffiti coating systems The obtained results of performed in 6 replication measurements results are grouped into 4 groups reflecting the adopted technological systems. The analysis covered 3 observed values: total surface free energy (TSFE), dispersive component of surface free energy (DC-TSFE) and polar component of surface free energy (PC-TSFE).

When comparing the mean values, the homogeneity of variance was checked using Le-ven's test. In the case of non-contradiction with the assumption of homogeneity of means, the classical ANOVA analysis of variance was performed with simultaneous determina-tion of homogeneous groups using the Tukey test. In the case of rejection of the hypothesis of homogeneity of means, the test of their

 doi:10.20944/preprints202505.0859.v1

equality was performed using the Welch test with simultaneous determination of homogeneous groups using the Games-Howell method.

The results of detailed statistical analyses performed for total surface free energy (TSFE), dispersive component of total surface free energy (DC-TSFE) and polar component of total surface free energy (PC-TSFE) are presented below.

a) Total surface free energy (TSFE).

Descriptive statistics for total surface free energy TSFE are presented in Table 5.

Table 5. Descriptive statistics for total surface free energy TSFE.

Coating system	Mean	SE Mean	StDev	Min.	Median	Max.
BO-100AGR	48.15	0.28	0.69	47.2	48.15	49.2
XPC60011	49.87	1.28	3.14	46.9	49.55	53.4
XPC60012	52.30	0.36	0.87	51.0	52.40	53.3
XPC60036	55.85	0.23	0.55	55.1	55.85	56.6

Leven's test of homogeneity of variance was performed, which rejected ($p < 0.001$) the hy-pothesis of equality of variances. An attempt to perform the Box-Cox transformation showed the optimal value of the parameter $\lambda>5$, which means that it is impossible to achieve variance stabilization in this way. Therefore, an assessment of the equality of mean values was performed using the Welch method, which rejected ($p < 0.001$) the hy-pothesis of equality of all mean values. Figure 5 presents a box plot of individual groups. Next, possible homogeneous groups were identified, i.e. sets of measured values that are statistically indistinguishable. Identification of homogeneous groups using the Games-Howell method showed the existence of 3 homogeneous groups, 2 of which over-lapped each other (Table 6).

Table 6. Total surface free energy TSFE homogeneous groups (95% confidence level).

Coating system	N	Mean	Grouping		
XPC60036	6	55.9	A		
XPC60012	6	52.3		B	
XPC60011	6	49.9		B	C
BO-100AGR	6	48.2			C

 doi:10.20944/preprints202505.0859.v1

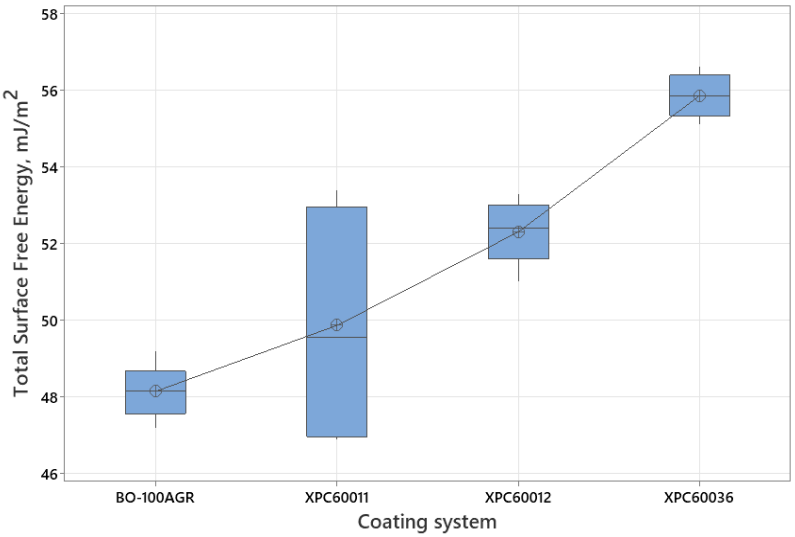

Figure 5. Distribution of total surface free energy TSFE values.

b) Dispersive component of total surface free energy (DC-TSFE).

Descriptive statistics for the dispersive component of the total surface free energy DC-TSFE are presented in Table 7.

Table 7. Descriptive statistics for the dispersive component of the total surface free energy DC-TSFE.

Coating system	Mean	SE Mean	StDev	Min.	Median	Max.
BO-100AGR	39.97	0.13	0.33	39.5	40.00	40.3
XPC60011	44.12	0.25	0.61	43.6	43.95	45.3
XPC60012	44.87	0.34	0.84	44.0	44.85	46.3
XPC60036	46.52	0.15	0.37	46.1	46.45	47.0

Leven's test of homogeneity of variance was performed, which not rejected the hypothesis of equality of variances ($p = 0.41$). Therefore, an assessment of the equality of mean values was performed using the classic ANOVA method, which rejected ($p < 0.001$) the hypothe-sis of equality of all mean values. Figure 6 presents a box plot of individual groups. Next, possible homogeneous groups were identified, i.e. sets of measured values that are statis-tically indistinguishable. Identification of homogeneous groups using the Tukey Pairwise Comparison method showed the existence of 3 non-overlapped homogeneous groups (Table 8).

Table 8. Dispersion component of the total surface free energy DC-TSFE homogeneous groups (95% confidence level).

Coating system	N	Mean	Grouping		
XPC60036	6	46.5	A		
XPC60012	6	44.9		B	
XPC60011	6	44.1		B	
BO-100AGR	6	40.0			C

 doi:10.20944/preprints202505.0859.v1

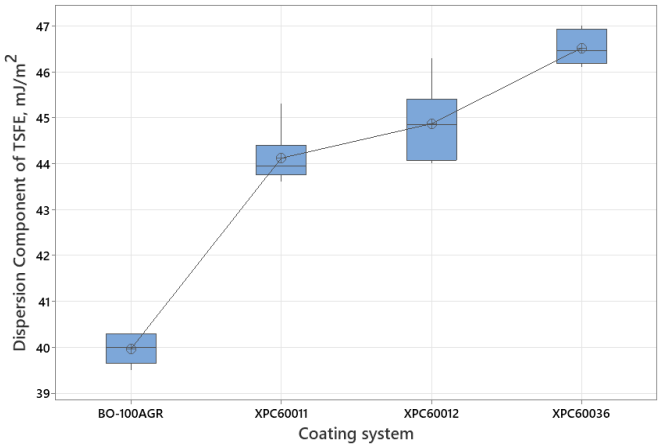

Figure 6. Distribution of the dispersive component of the total surface free energy DC-TSFE values.

c) Polar component of total surface free energy (PC-TSFE)

Descriptive statistics for the polar component of the total surface free energy PC-TSFE are presented in Table 9.

Table 9. Descriptive statistics for the polar component of the total surface free energy PC-TSFE.

Coating system	Mean	SE Mean	StDev	Min.	Median	Max.
BO-100AGR	8.20	0.30	0.73	6.9	8.25	9.1
XPC60011	5.78	1.17	2.88	3.1	5.65	8.8
XPC60012	7.45	0.35	0.85	5.9	7.75	8.2
XPC60036	9.33	0.13	0.31	8.9	9.35	9.8

Leven's test of homogeneity of variance was performed, which rejected ($p < 0.001$) the hy-pothesis of equality of variances. An attempt to perform the Box-Cox transformation showed the optimal value of the parameter λ=4, however, after its execution, the Leven test still indicated the lack of homogeneity of variance ($p = 0.005$). Therefore, an assessment of the equality of mean values was performed using the Welch method, which rejected ($p < 0.001$) the hypothesis of equality of all mean values. Figure 7 presents a box plot of indi-vidual groups. Next, possible homogeneous groups were identified, i.e. sets of measured values that are statistically indistinguishable. Identification of homogeneous groups using the Games-Howell method showed the existence of 2 homogeneous nonoverlapped groups (Table 10).

Table 10. Polar component of the total surface free energy PC-TSFE homogeneous groups (95% confidence level).

Coating system	N	Mean	Grouping	
XPC60036	6	9.33	A	
XPC60012	6	8.20		B
XPC60011	6	7.45		B
BO-100AGR	6	5.78		B

 doi:10.20944/preprints202505.0859.v1

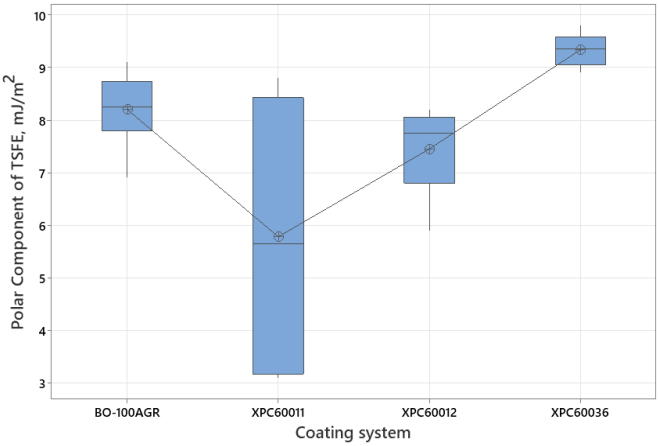

Figure 7. Distribution of the dispersive component of the total surface free energy DC-TSFE values.

3.2.3. Measurements of the geometric structure of the surface

The geometric structure of the surface has a significant impact on many processes occurring in the surface layer and is one of the most important factors determining its quality values. It has a significant impact on the operational properties of machine elements, which include, for example: friction conditions on the contact surfaces of the mating elements, contact stresses, fatigue strength, corrosion resistance, tightness of connections, surface thermal radiation and magnetic properties. The problems of measurement methods and the assessment of surface roughness and waviness are discussed in the articles [31-33]. The used measuring devices and and method of test speciments preparation are described in detail in the article [30].

Comparison of surface roughness are visualized for selected single measurements for the tested anti-graffiti coatings are shown in Fig. 8. Comparison of surface waviness are visualized for selected single measurements are shown in Fig. 9. While in Fig. 10 they are shown elevation distribution and load-bearing capacity curves of the roughness for tested anti-graffiti coatings (results of analysis of roughness).

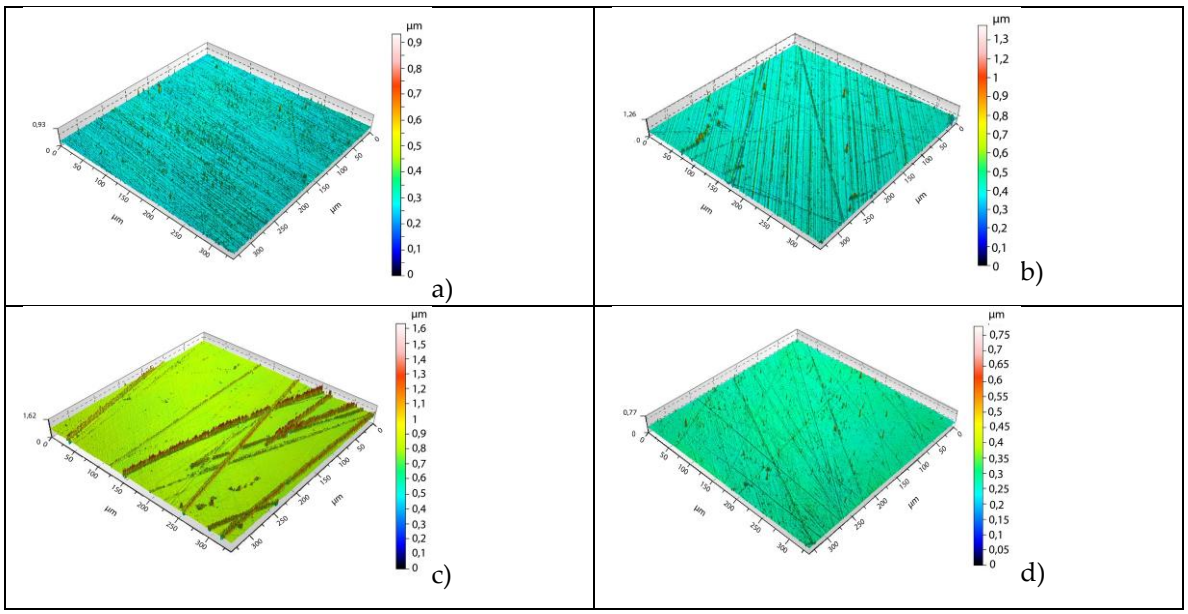

Figure 8. Surface roughness for the anti-graffiti coatings: a) XPC 60012, b) XPC 60036, c) XPC 60011, d) BO100-AGR .

 doi:10.20944/preprints202505.0859.v1

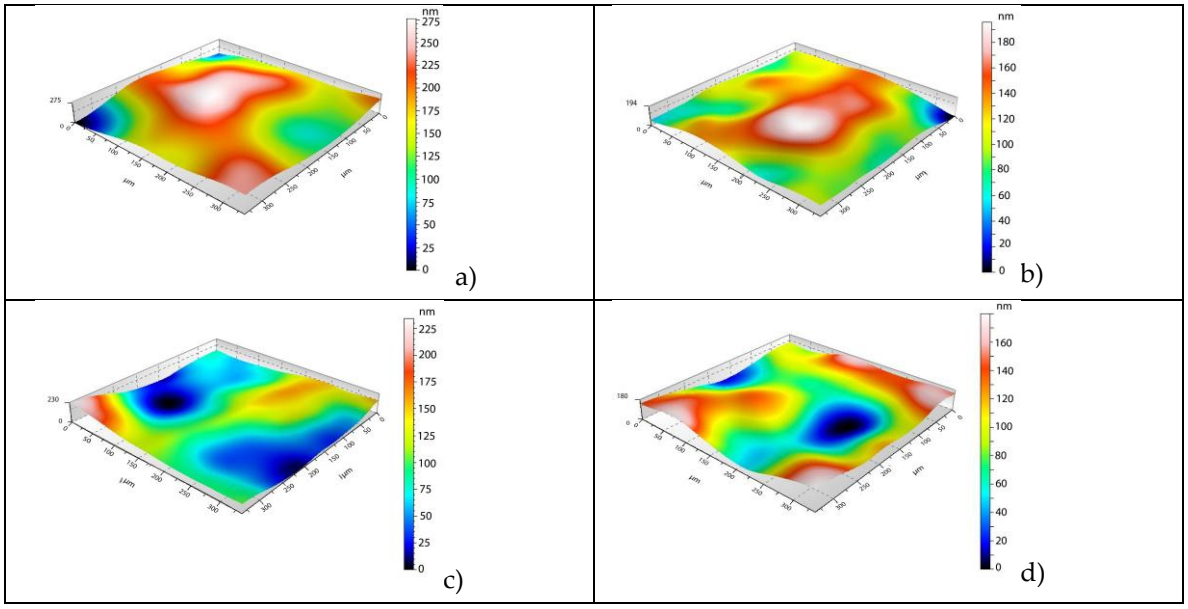

Figure 9. Surface waviness for the anti-graffiti coatings: a) XPC 60012, b) XPC 60036, c) XPC 60011, d) BO100-AGR .

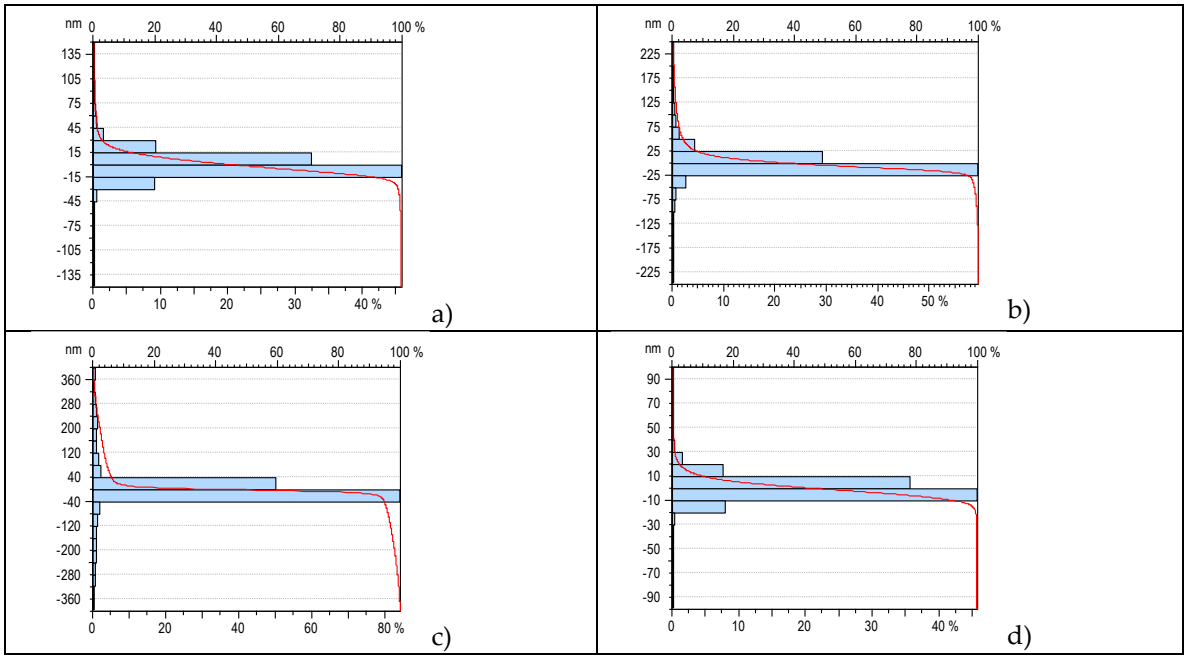

Figure 10. Elevation distribution and load-bearing capacity curves of the roughness for the anti-graffiti coatings: a) XPC 60012, b) XPC 60036, c) XPC 60011, d) BO100-AGR .

3.2.4. Adhesion

The adhesion results of the coating systems were similar to each other. From the test results obtained, the XPC 60011 anti-graffiti coating system (2.28 MPa) had the highest average adhesion value. The XPC 60012 paint system (2.18 MPa) characterized by the lowest average adhesion value had a 5% lower adhesion, compared to the XPC 60011 coating system.

The adhesion results obtained were characterized by low standard deviation values, indicating the high repeatability of the test performed. Measurement of adhesion by the peel method after the test cycle in the aging chambers was also performed. The obtained adhesion results along with the standard deviation are summarized in Table 11. Figure 11 shows the sample after the adhesion test.

 doi:10.20944/preprints202505.0859.v1

Table 11. Values of chosen parameters of adhesiveness (MPa) obtained by the peel-off method

Coating system	Average value	Standard deviation	Range
XPC 60011	2.28	0.14	0.38
XPC 60012	2.18	0.08	0.25
XPC 60036	2.24	0.07	0.19
BO100-AGR	2.22	0.07	0.18

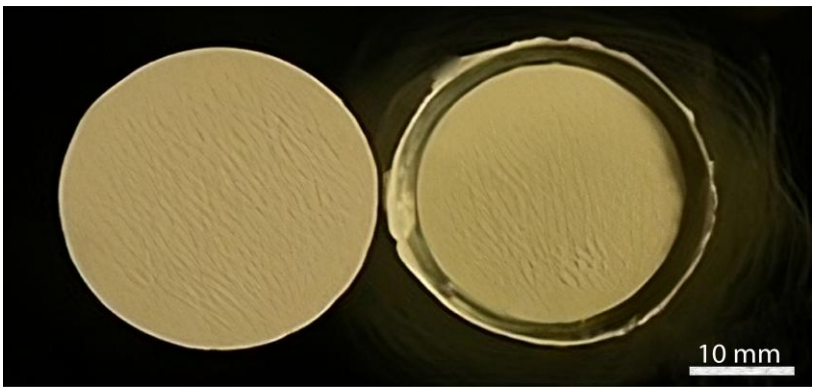

Figure 11. View of sample after adhesion test of XPC 60012 coating system.

Significantly greater differences in adhesion values were observed between the tested systems after exposing the samples to condensation moisture. The XPC 60011 anti-graffiti coating system had the highest adhesion value of 2.23 MPa, compared to the system with the lowest adhesion value of 2.02 MPa (BO100-AGR). The percentage change in adhesion value with respect to the initial value before exposure was also calculated. In this case, the XPC 60011 coating system also had the smallest change, with a reduced adhesion of 2.34%. Such a small change can be considered a measurement error. On the other hand, the largest change in adhesion was observed for the XPC60036 anti-graffiti coating system, a reduction in adhesion of 9.73% compared to the initial value was recorded.

3.2.5. Nanohardness

The production of coatings with the required micromechanical properties is a major research challenge. In the production process, it is necessary to determine the controlled parameters and properties that we expect from the resulting coating. The multitude of controlled parameters and their values means that a large number of combinations affects high costs. In our case, we investigated the nanohardness and the modulus of longitudinal elasticity (Young's modulus) of anti-graffiti coating systems.

Nanohardness and Young's modulus measurements were performed using a NANOVEA nanohardness tester. The nanohardness tester consists of a Berkovich indenter, an optical microscope and a motorized stage in the X and Y axes. Precise determination of the measurement location is possible thanks to the sample positioning system with an accuracy of 1 μm. Additionally, which is particularly important when testing thin layers, the force is measured with an accuracy of 0.01 mN, and the indenter penetration is up to 10 nm. The device allows for measurements using an indentation force from 1 mN to 400 mN.

Nanohardness and Young's modulus of the tested samples were measured on the surface in the anti-graffiti paint layer and on the cross-sections of the coating system (mixed sections) in each layer, i.e. anti-graffiti layer, base layer, primer layer, filler and substrate material (S355 steel). The tests were performed with the following parameters: linear load, max. load 3 mN, load and unload speed 40 mN/min and the break time between subsequent load and unload cycles 3 s. The average values of nanohardness and Young's modulus were determined based on 10 measurements.

 doi:10.20944/preprints202505.0859.v1

Nanohardness was determined as the indenter penetration depth, while the modulus of elasticity was determined by the slope of the unloading curve. The results of nanohardness and Young's modulus measurements are presented in Table 12.

Table 12. Average values of nanohardness and modulus of elasticity in the anti-graffiti coating measured on the surface

Materials	Nanohardness (GPa)	Young's modulus (GPa)
XPC 60012	0.23 ± 0.01	2.70 ± 0.05
BO100-AGR	0.26 ± 0.01	2.90 ± 0.02
XPC 60011	0.27 ± 0.01	2.84 ± 0.04
XPC 60036	0.26 ± 0.01	2.84 ± 0.03
Steel S355	10.60 ± 0.70	124.00 ± 5.30

The highest nanohardness was found in the S355 alloy steel. which was 10.6 GPa. The Young's modulus was also the highest for the S355 steel. at 124 GPa. Analyzing the data in Table 10 it can be concluded that all anti-graffiti paint coatings had similar nanohardness values. The nanohardness measured on the surface of the anti-graffiti coatings was in the range of 0.229 GPa to 0.265 GPa.

A similar analogy can be observed when analyzing the values of Young's moduli for the tested anti-graffiti paint layers (Table 12). The highest value of the longitudinal modulus of elasticity was found in the BO100-AGR anti-graffiti paint layer compared to the other three anti-graffiti paint layers. The Young's modulus measured on the surface of the BO100-AGR layer was 2.900 GPa. The XPC 60012, XPC 60011, XPC 60036 paint layers had Young's modulus values in the range of 2.700-2.843 GPa (measured on the surface of the coating). The greater elasticity of the BO100-AGR anti-graffiti top layer compared to the other three anti-graffiti paint layers may result from the additives that make up its chemical composition. Example views of the indenter impressions are shown in Fig. 12.

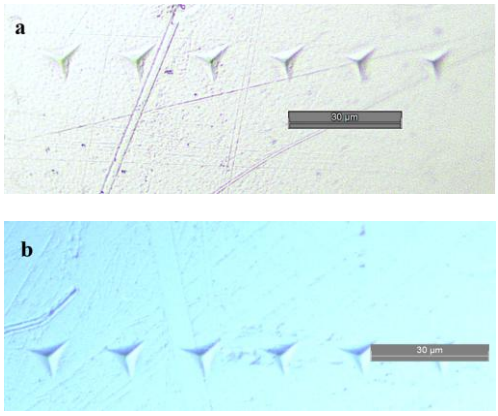

Figure 12. Indentation marks during nano-hardness measurements on the surface of anti-graffiti paint coating: a) BO100-AGR, b) XPC 60036

The obtained results of nanohardness and Young's modulus measurements show that the anti-graffiti paint coatings were characterized by high homogeneity and the absence of defects in their structure, e.g. the absence of pores and microcracks.

3.2.6. Hardness

The hardness measurement consisted of measuring the damping time of the pendulum according to the standard PN-EN ISO 1522 [34]. The sample was placed on the table of the device.

 doi:10.20944/preprints202505.0859.v1

and then the pendulum legs were gently positioned on its surface. A Koenig pendulum was used in the tests. During the measurement the number of oscillations over time with damped vibrations of the pendulum from the initial yaw angle of 6 deg to a final angle of 3 deg from vertical was counted. The photocell in the device was responsible for the correct number of counts. The number of oscillations was converted to pendulum damping time. In a properly calibrated device using a Koenig pendulum. time of one oscillation should be about 1.4 s. The measurement was carried out six times on each sample. in order to average the hardness according to the thickness of the coating. The principle of the measurement was to change the friction surface between the coating under test and the pendulum legs. which translates into the damping time of the pendulum. Coatings with lower hardness more easily yield to the weight of the pendulum. whose legs penetrate the coating more deeply. resulting in an increase in the friction surface. Hardness measurements were also made after exposing the samples to aging chambers. The initial results and the results obtained after testing in the salt chamber and humidity chamber are shown in Table 13. The results shown are the averages of 6 measurements. The method is characterized by high repeatability and reproducibility of results.

Table 13. Hardness measurement results according to PN-EN ISO 1522 – Koenig pendulum

Coating system	Damping time (s)	Relative hardness (-)	Damping time – salt (s)	Damping time – humidity (s)
XPC 60011	95.2	0.4	140.0	146.7
XPC 60012	83.7	0.3	135.0	150.9
XPC 60036	109.8	0.4	132.2	145.9
BO100-AGR	120.8	0.5	134.4	147.8

Individual results may change slightly in cyclic tests. Therefore. a relative hardness was introduced. which is calculated by dividing the oscillation value of the sample by the oscillation value of the calibration. The preceding calibration measurement ended with a value of 180 oscillations. Relative hardness values are also shown in Table 11 for comparison of each system. The XPC 60012 anti-graffiti coating system had the lowest oscillation damping value (83.7 s). compared to the BO100-AGR coating system. with the highest oscillation damping time (120.8 s). An increase in the hardness of the anti-graffiti coating systems was observed after aging tests in the salt chamber and humidity chamber. All tested coating systems were characterized by high damping times falling within the range of 132-140 s. When measured after the salt chamber tests. the largest increase (by 162% of the initial value) in damping time was obtained for the XPC 60012 coating system. while the XPC 60011 anti-graffiti coating system had the highest hardness corresponding to 140 s of test duration. After the test in the humidity chamber. the paint systems also had high and similar pendulum damping time values (146-150 s). The XPC 60012 anti-graffiti coating system had the highest hardness after completed exposure to moisture. while the lowest average result was completed for the XPC 60036 coating system. Aging tests were conducted at elevated temperatures (313 K). The test conditions in the aging chambers may have accelerated the evaporation of solvents that remained in the individual layers after the conditioning period. During the drying process of the anti-corrosion primer. about 95% of the solvents evaporate from the primer layer. with the remaining 5% evaporating over a period of up to 3 weeks. Applying another layer of the coating system over the anticorrosive primer will extend this time significantly. The remaining small amount of solvent in each layer of the system translates into hardness by the pendulum damping method. Placing the samples in an aging chamber at an elevated temperature for the duration of the hardness test accelerated the migration of the remaining solvents in the system affecting its hardness.

3.3. Method of material selection

Proper selection of materials for the manufacture of protective anti-graffiti coating systems makes it possible to meet the expectations of the railway users. Therefore, a method was proposed to

 doi:10.20944/preprints202505.0859.v1

facilitate the selection process. An optimization method was used by formulating a generalized objective function. The method was applied to the selection of clear anti-graffiti coating in the railroad industry. The same anti-graffiti coating systems as used in described above laboratory tests were considered: BO100-AGR (produced by F.H. BARWA), XPC 60011, XPC 60012 and XPC 60036 (produced by PPG).

During the realisation of the PhD thesis [5], some experiments were conducted on the removal of graffiti from previously painted railway wagons with selected BARWA products. Based on their results and experience, the following parameters were assumed as input variables of the model: adhesion (d_1), surface free energy (d_2), corrosion current density (d_3), scratching (d_4), pendulum damping time (d_5). Moreover material price (d_6) was taken into account. The cost of technology and application are omitted. In the experimental studies, all tested paint systems were applied to vehicles under the same conditions (in particular, at the same air pressure, working medium pressure and annealing temperature). For the quantitative evaluation of individual criteria, a rating scale ranging from zero to one ($d_i \in [0,1]$, i=1,...,6) was adopted, indicatively taking the following values for their descriptive status (selection scale):

very good - $d_i \in [0.8\text{-}1.0]$; $d_i=1$ - excellent;
good - $d_i \in [0.6\text{-}0.8)$;
sufficient - $d_i \in [0.4\text{-}0.6)$;
bad - $d_i \in [0.2\text{-}0.4)$;
very bad - $d_i \in [0\text{-}0.2)$; di=0 – unacceptable.

The range of values of variables from zero to one corresponds to the range of values of these variables that are obtainable, or are acceptable in practical applications (due to technological capabilities and cost).

Based on the obtained d_i subgrades, the resulting value of the total quality function D is defined as the geometric mean of the subfunctions (2). The value of the D function is also in the range $D \in [0,1]$.

$$D = \sqrt[6]{d_1 \cdot d_2 \cdots d_6} \qquad (2)$$

The values of the partial quality functions obtained from the analyses of coatings made with selected anti-graffiti coating systems and the corresponding values of the total quality functions D are summarized in Table 2.

Table 2. Partial and total quality functions for tested anti-graffiti coating systems

Quality function	XPC60011	XPC60012	XPC60036	BO100-AGR
d_1	0.73	0.69	0.72	0.71
d_2	0.81	0.68	0.42	0.87
d_3	0.81	0.81	0.80	0.81
d_4	0.53	0.55	0.55	0.62
d_5	0.25	0.21	0.56	0.42
d_6	0.66	0.88	0.81	0.75
D	0.59	0.43	0.63	0.68

Based on the calculations, it is possible to compare selected anti-graffiti coating systems used in the rail vehicle industry. The best parameters were possessed by the BO100-AGR anti-graffiti coating system. All the tested coating systems showed similar parameters of adhesion to the surface of the substrate material and corrosion resistance measured by corrosion current density. The largest difference between the tested systems was observed for the parameters of surface free energy and hardness evaluated through pendulum damping time. It is also possible to distinguish coating systems with significant hardness (BO100-AGR and XPC 60036) and coating systems with lower surface free energy (XPC 60011 and BO100-AGR).

 doi:10.20944/preprints202505.0859.v1

4. Discussion

The conducted studies indicate that modification of the surface layer to reduce its surface free energy contributes to obtaining protective coating systems for special applica-tions. Coating systems prepared in this way are characterized by reduced adhesion of unwanted substances on its surface. Unwanted substances on the surface layer of a coating system are various types of operational dirt and man-made contaminants such as graffiti. Reduced adhesion also allows easier and faster removal of water droplets with chemically active substances dissolved in them from the surface of the coating under the action of gravity. The use of a modified anti-graffiti coating does not reflect negatively on the properties of the entire paint system. The protective system retains its mechanical properties such as hardness. adhesion and scratch resistance. Also. the modified top coat does not negatively affect the protective system's UV-B resistance. condensation moisture resistance and corrosion resistance.

Modification of the surface tension of the antigraffiti coating in the liquid phase prior to application to vehicle surfaces has a very positive effect on its spreadability. which translates into low roughness of the resulting surface layer. Small values of roughness af-fect the reduction of adhesion forces by reducing the specific surface area contacting the anti-graffiti protective coating with unwanted contaminants.

A very important factor affecting the geometric structure of the coating system is the proper preparation of the substrate material. Paint systems are characterized by lower roughness in relation to the substrate material (two orders of magnitude). In addition. the isometric images of the coating systems show traces of the preceding treatment. which was sanding.

The XPC 60011 anti-graffiti coating system has the highest adhesion. while the XPC 60012 paint system has the lowest adhesion.

The BO100-AGR anti-graffiti coating system has similar mechanical properties with respect to the anti-graffiti coating systems of a foreign manufacturer (PPG).

Economic considerations and environmental requirements make it necessary to int-roduce new solutions that ensure a reduction in unit manufacturing costs while ensuring the quality of the produced paint systems. The physical properties of the surface layer are important due to the stability of the technological process using the phenomenon of adhe-sion.

A multifaceted approach to counteract the formation of graffiti on railroad cars re-quires the following measures:

- Investment in equipping the rail base with a system of monitoring and protection of railroads using modern technologies;
- Organization of preventive measures in the form of patrols specializing in chasing graffiti artists during the day;
- Organization of security services including night patrols with the use of advanced technologies. including surprise actions involving the organization of so-called “ambushes”. in places where railway depots spend the night;
- Widespread implementation of the procedure for identifying and removing graffiti from railroad cars. especially in the context of removing the graffiti coating as soon as possible.

5. Conclusions

1. Railway companies need protection systems for their vehicles and wagons.
2. The BO100-AGR anti-graffiti coating system was characterized by similar mechani-cal properties to the anti-graffiti coating systems of a foreign manufacturer (PPG).
3. The analysis of the microstructure showed that the thickness of the anti-graffiti coat-ing systems was in the range of 2300-2400 μm. Moreover, the paint systems were free of pores and micro-cracks.

 doi:10.20944/preprints202505.0859.v1

4. The BO100-AGR anti-graffiti coating system had the lowest free surface energy. Compared to the other three anti-graffiti coating systems, the BO100-AGR paint sys-tem had the best anti-adhesive properties. The anti-adhesive properties of the BO100-AGR system may be of great importance in a potential application on rail ve-hicles.
5. Economic considerations make it necessary to introduce new solutions that ensure the reduction of unit manufacturing costs while ensuring the quality of the produced paint systems. The physical properties of the surface layer are important due to the stability of the technological process using the phenomenon of adhesion.
6. It is necessary to strictly maintain quality requirements both in the preparation of an-ti-graffiti coatings and in their removal.
7. The use of anti-graffiti coatings reduces the negative impact on the environment with a view to reducing the negative impact on the ecosystem.
8. An alternative method of vehicle skin protection that is currently possible is to cover vehicles with a special film. which significantly increases anti-graffiti protection. According to the manufacturer's declaration. the special film guarantees a seven-year warranty on the material. as well as no limit on the number of graffiti removals when using dedicated agents for this process.

Author Contributions: For research articles with several authors, a short paragraph specifying their individual contributions must be provided. The following statements should be used "Conceptualization, E.K., M.K. and N.R.; methodology, E.K. and N.R.; software, Ł.P.; validation, Ł.O. and N.R.; formal analysis, Ł.O.; investigation, E.K. and N.R.; resources, E.K., N.R. and Ł.P.; data curation, N.R. and Ł.P.; writing—original draft preparation, E.K., Ł.O. and N.R.; writing—review and editing, M.K.; visualization, Ł.P.; supervision, M.K. and N.R.; project administration, N.R.; funding acquisition, MK

Funding: This research received no external funding.

Institutional Review Board Statement: Not applicable.

Informed Consent Statement: Not applicable.

Data Availability Statement: The data presented in this study are available on request from the corresponding author.

Acknowledgments: The authors would like to thank Mr. Mariusz Sowiński, Deputy Director, Rolling Stock Maintenance Department, Małopolska Railways Ltd. for providing information on the prevention and removal of graffiti from railcars and their costs in the company.

Conflicts of Interest: The authors declare no conflicts of interest.

References

1. Vega-Bosh, A.; Santamarina-Campos, V.; Bosh-Roig, P. Assessing the Feasibility of Removing Graffiti from Railway Vehicles Using Ultra-Freezing Air Projection. *Appl. Sci.* **2024**. 14(10). 4165. https://doi.org/10.3390/app14104165.
2. Pietrzak, A.; Ulewicz, M.; Kozień, E.; Pietraszek, J. Application of a Mixture of Fly Ash and Solid Waste from Gas Treatment from Municipal Solid Waste Incineration in Cement Mortar. *Materials* **2025**. 18, 481. https://doi.org/10.3390/ma18030481.
3. Można poradzić sobie z graffiti. choć to walka nie tylko z spreyowcami. ale także silna konkurencja pomiędzy producentami farb i powłok antygraffiti. Available online: https://www.skm.warszawa.pl/mozna-poradzic-sobie-z-graffiti-choc-to-walka-nie-tylko-ze-spreyowcami-ale-takze-silna-konkurencja-pomiedzy-producentami-farb-i-powlok-antygraffiti-od-lat-tocza-miedzy-soba-wojne-o-zwyciestwo-a-za-2/ (accessed on 15.04.2024).
4. Salamon, P. Małopolska zamawia nowe pociągi: z powłoką antygraffiti. Available online: https://lovekrakow.pl/aktualnosci/malopolska-zamawia-nowe-pociagi-z-powloka-antygraffiti_33921.html (accessed on 15.04.2024).
5. Pasieczyński, Ł. Performance properties of anti-graffiti coating systems for railway rolling stock. PhD Dissertation, Kielce University of Technology, Kielce, Poland, 2019.

 doi:10.20944/preprints202505.0859.v1

6. Radek, N. Properties of WC-Co coatings with Al_2O_3 addition. *Production Engineering Archives* **2023**. 29(1). 94-100. https://doi.org/10.30657/pea.2023.29.11.
7. Burakowski, T.; Wierzchoń, T. *Inżynieria powierzchni metali*; WNT: Warszawa. Poland. 1995.
8. Batchelor, A.W.; Stachowiak, G.W. Predicting synergism between corrosion and abrasive wear. *Wear* **1988**. 123. 281-291. https://doi.org/10.1016/0043-1648(88)90144-5.
9. Radek, N.; Michalski, M.; Mazurczuk, R.; Szczodrowska, B.; Plebankiewicz, I.; Szczepaniak, M. Operational tests of coating systems in military technology applications. *Eksploatacja i Niezawodnosc - Maintenance and Reliability* **2023**. 25(1). 12. http://doi.org/10.17531/ein.2023.1.12.
10. Decker, C.; Balandier, M. Degradation of poli(vinyl chloride) by U.V. radiation – I. Kinetics and quantum yields. *European Polymer Journal* **1982**. 18. 1085-1091. https://doi.org/10.1016/0014-3057(82)90209-9.
11. Decker, C.; Biry, S. Light stabilization of polymers by radiation-cured acrylic coatings. *Progress in Organic Coatings* **1996**. 29(1-4). 81-87. https://doi.org/10.1016/S0300-9440(96)00630-3.
12. Kotnarowska, D. Influence of Ultraviolet Radiation on Erosive Resistance of Modified Epoxy Coatings. *Solid State Phenomena* **2006**. 113. 585-588. https://doi.org/10.4028/www.scientific.net/SSP.113.583.
13. Kotnarowska, D. Analysis of polyurethane top-coat destruction influence on erosion kinetics of polyurethane-epoxy coating system. *Eksploatacja i Niezawodność - Maintenance and Reliability* **2019**. 21(1). 103-114. http://doi.org/10.17531/ein.2019.1.12.
14. Kotnarowska, D. Influence of ultraviolet radiation and aggressive media on epoxy coating degradation. *Progress in Organic Coatings* **1999**. 37(3-4). 149-159. http://doi.org/10.1016/S0300-9440(99)00070-3.
15. Kazicyna, L.A.; Kupletska, N.B. *Metody spektroskopowe wyznaczania struktury związków organicznych*; PWN: Warszawa. Poland. 1976.
16. Dobrzański, L. *Podstawy nauki o materiałach i metaloznawstwo;* Wydawnictwo Naukowo Techniczne: Warszawa. Poland. 2002.
17. Nguyen, T.; Bentz, D.; Byrd, E. Method for measuring water diffusion in a coating applied to a substrate. *Journal of Coatings Technology* **1995**. 67(844). 37-46.
18. Nguyen, T.; Hubbard, J.B.; Pommersheim, J.M. Unified model for the degradation of organic coatings on steel in a neutral electro-lyte. *Journal of Coatings Technology* **1996**. 68(855). 45-56.
19. Sokólski, W. Światowa Organizacja Korozji – geneza powstania. misja i cele. program działania. *Ochrona przed korozją* **2009**. 9. Polskie Stowarzyszenie Korozyjne. Gdańsk.
20. Kotnarowska, D. Destruction of Epoxy Coatings under the Influence of Sodium Chloride Water Solutions. *Solid State Phenomena* **2015**. 220-221. 609-614. http://doi.org/10.4028/www.scientific.net/SSP.220-221.609.
21. Kohl, M.; Kalendova, A. Anticorrosion properties of organic coatings containing polyphenylenediamine phosphate. *Advances in Sciences and Technology Research Journal* **2015**. 9(29). 47-50. http://doi.org/10.12913/22998624/60782.
22. Mróz, A.; Szymański, M.; Koch, P.; Pawlicki, M.; Meller, A.; Przekop, R.E. The Influence of Surface Texture of Elements Made of PA6-Based Composites on Anti-Graffiti Effect of Paint Coating. *Materials* **2024**. 17(9). 1951. https://doi.org/10.3390/ma17091951.
23. Bartman, M.; Balicki, S.; Wilk, K.A. Formulation of Environmentally Safe Graffiti Remover Containing Esterified Plant Oils and Sugar Surfactant. *Molecules* **2021**. 26. 4706. https://doi.org/10.3390/molecules26154706.
24. Graffiti – kosztowny wandalizm. Available online: https://wiadomosci.wp.pl/graffiti-kosztowny-wandalizm-6109012257666177a (accessed on 15.04.2024).
25. Włuka, E. Jak przewoźnicy radzą sobie z wandalizmem? Available online: https://zbiorowy.info/2018/11/jak-przewoznicy-radza-sobie-z-wandalizmem/ (accessed on 15.04.2024).
26. Wandalizm graffiti na pociągach Renfe wygenerował koszty w wysokości ponad 25 milionów euro. Available online: https://kurier-kolejowy.pl/aktualnosci/41870/wandalizm-graffiti-na-pociagach-renfe-wygenerowal-koszty-w-wysokosci-ponad-25-milionow-euro.html (accessed on 15.04.2024).
27. Akt wandalizmu sparaliżował metro. Available online: https://haloursynow.pl/pl/11_wiadomosci/784_stolica/21767_akt-wandalizmu-sparalizowal-metro-zaciagneli-hamulec.html (accessed on 15.04.2024).

 doi:10.20944/preprints202505.0859.v1

28. Wierzbicki, P. Szok w warszawskim metrze. Available online: https://www.fakt.pl/wydarzenia/polska/warszawa/groza-w-warszawskim-metrze-zatrzymali-pociag-pasazerowie-byli-przerazeni/x1pr6hl (accessed on 15.04.2024).
29. Szokujące sceny z warszawskiego metra. Available online: https://www.fakt.pl/wydarzenia/polska/warszawa/szokujace-sceny-z-warszawskiego-metra-nikt-nie-przeszkodzil-wandalom/qqcve5k (accessed on 15.04.2024).
30. Radek, N.; Pasieczyński, Ł.; Pietraszek, J.; Broncek, J. Analysis of the surface geometric structure of the anti-graffiti coating systems intended for rolling stock. *Mechanik* **2019**. 2. 124-127. https://doi.org/10.17814/mechanik.2019.2.21.
31. Adamczak, S.; Makieła, W. Analyzing variations in roundness profile parameters during the wavelet decomposition process using the matlab environment. *Metrology and Measurement Systems* **2011**. XVIII(1). 25-34.
32. Miller, T.; Adamczak, S.; Świderski, J.; Wieczorowski, M.; Łętocha, A.; Gapiński, B. Influence of temperature gradient on surface texture measurements with the use of profilometry. *Bulletin of the Polish Academy of Sciences* **2017**. 65(1). 53-61.
33. Oczoś, K.; Lubimov, V. *Struktura geometryczna powierzchni*; Wydawnictwo Politechniki Rzeszowskiej: Rzeszów. Poland. 2003.
34. PN-EN ISO 1522:2008: Farby i lakiery - Badanie metodą tłumienia wahadła.